

Heterogeneously Integrated Near-Infrared DFB Laser on Tantalum Pentoxide

Ali Eshaghian Dorche^{1,2,*}, Nima Nader^{2,*}, Eric J. Stanton^{1,2}, Sae Woo Nam², Richard P. Mirin²

¹ Department of Physics, University of Colorado, 2000 Colorado Avenue, Boulder, Colorado 80309, USA

² Applied Physics Division, National Institute of Standards and Technology, Boulder CO 80305, USA

Corresponding author email: ali.eshaghianandorche@nist.gov, nima.nader@nist.gov

Abstract: We present a diode laser heterogeneously integrated with tantalum pentoxide waveguides on a silicon substrate emitting 5 mW continuous-wave power per facet at 1020 nm wavelength with a 14 mA threshold and a 22 dB side-mode-suppression ratio.

OCIS codes: (230.5590) Quantum-well, -wire and -dot devices; (140.5960) Semiconductor lasers; (160.3130) Integrated optics materials

1. Introduction

Heterogeneous integration of group III-V based quantum well or quantum dot active regions with passive integrated photonic circuitry is a necessary step toward making scalable and stand-alone optical systems with low-cost and small form factors [1]. Such monolithic platforms would enable the generation, amplification, manipulation, and detection of coherent light signals for custom applications at desired wavelengths. Applications leveraging such a platform are versatile, ranging from precise measurement, atomic clocks, and sensing to classical or quantum information processing, and optical interconnects for data centers and telecommunications. Thanks to the telecommunication applications and the maturity of Si photonic integrated circuitry (PIC), most of the focus on developing heterogeneous diode lasers has been on wavelengths above the Si bandgap, mainly in the O- and C-bands [2, 3]. Nonetheless, with increasing interest for applications at wavelengths below the Si bandgap (e.g., quantum information processing, quantum sensing, atom-photon chips, etc.), it is necessary to replace the Si, or hybrid SiN/Si, Lithium Niobate/Si platforms with large bandgap materials such as Si₃N₄ or tantalum pentoxide (tantala, Ta₂O₅).

In this paper, we present the first heterogeneously integrated distributed feedback (DFB) laser with an InGaAs quantum well active layer bonded directly on a patterned tantala laser cavity. Compared to low-loss stoichiometric LPCVD-Si₃N₄ previously used in heterogeneous diode lasers at near-infrared wavelengths [4], tantala has a lower thermo-optic coefficient and lower residual stress while enabling comparable low-loss PICs with high quality-factor microring resonators at near-infrared wavelengths below the Si bandgap [5, 6].

2. Fabrication

The InGaAs epitaxial layer stack, grown using molecular beam epitaxy (MBE) on a GaAs substrate, contains two 8 nm In_{0.21}Ga_{0.79}As quantum wells (QWs) separated by 10 nm GaAs barriers to form the active layers. The *p*- and *n*-doped contact layers are GaAs:Be, and GaAs:Si, and are grown as the top and bottom layers of the epi stack, respectively, in Fig. 1(a). A relatively thick layer of *p*-Al_{0.6}Ga_{0.4}As (800 nm) and a graded-index separate confinement heterostructure (GRINSCH) are grown on top of the QWs to vertically confine the optical mode at the vicinity of QWs, decreasing the mode overlap with the *p*-contact layer while increasing the total gain and providing an evanescent interaction with the underlying tantala PIC.

The DFB grating structure that forms the laser cavity is etched in a 300 nm thick tantala layer that is sputtered on a thermally oxidized Si wafer with an SiO₂ bottom cladding thickness of 800 nm. The pattern is first written in a ZEP 520 positive-tone resist using electron beam lithography (EBL) and is subsequently transferred to the tantala film using an inductively coupled plasma reactive-ion-etcher (ICP-RIE) using CHF₃/CF₄/Ar chemistry. The etch depth into the tantala layer is approximately 100 nm, which corresponds to a grating strength of $\kappa = 47 \text{ cm}^{-1}$. After etching, the tantala wafer is annealed at 500 °C in a pure dry air ambient for 5 hours to improve the optical quality of the film, motivated by empirical evidence from [5]. The 76 mm diameter epi-wafer is then directly bonded to the patterned tantala on Si wafer after depositing a few nanometers of alumina with atomic layer deposition and O₂ plasma activation of the bonding surfaces. Figure 1(b) shows an image of the bonded III-V epi-layer to the patterned tantala wafer with high area yield, after aqueous removal of the GaAs backside wafer with NH₄OH/H₂O₂ chemistry.

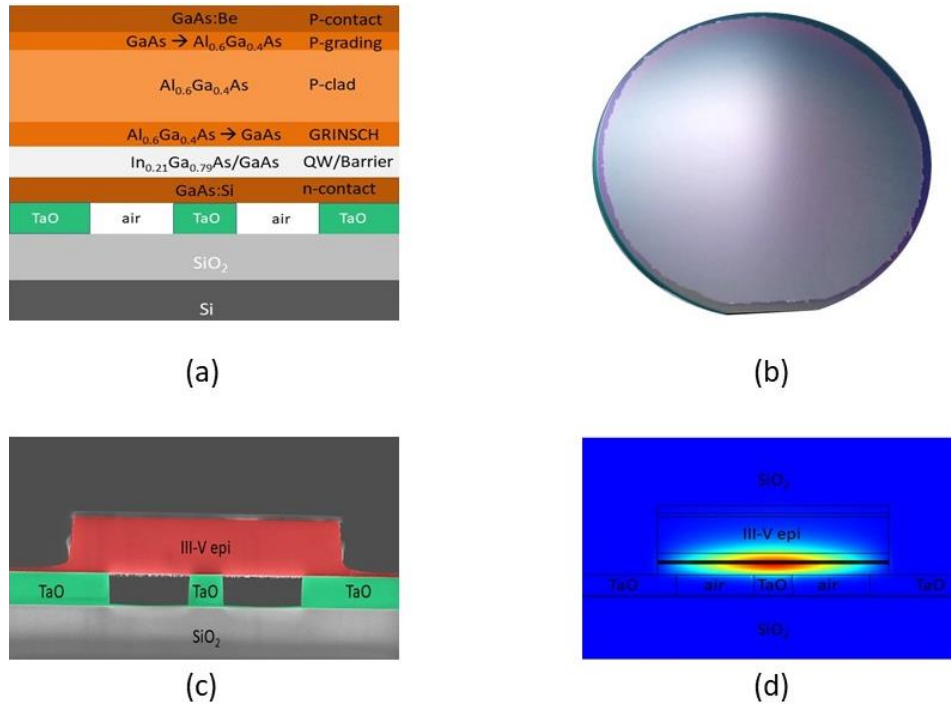


Figure 1. Details of direct wafer bonding of III-V InGaAs active layer to patterned tantalum PIC. a) Layers of the III-V active layer. b) Bonded wafers after backside removal to remove the GaAs substrate and the sacrificial etch-stop layer. (c) Cross-sectional scanning electron micrograph with false-color addition to highlight the III-V and tantalum layers. (d) Laser waveguide transverse-mode electric field profile showing strong overlap with the quantum-well layers.

The laser fabrication process is followed by EBL-patterning (using negative-tone resist) and etching of the laser mesas using SiCl_4/Ar chemistry. The laser-mesa etch is stopped after etching a few nanometers into the GaAs:Si n -contact layer. The n -contact is also patterned and etched to ensure there is no III-V slab left. After making ohmic contacts to the n -doped GaAs, using electron-beam evaporated Pd/Ge/Au metal stack, the SiO_2 top clad is deposited in an ICP-CVD chamber. Vias are opened in the top-cladding to deposit electron-beam evaporated Ti/Au p -contact on the p -doped GaAs, followed by probe metallization. The dies including DFB laser bars are diced and polished for further characterization.

Figure 1(c) represents the false-color cross-sectional scanning electron micrograph of the active layer bonded on the patterned tantalum waveguide layer after the laser mesa etch. The electric field profile of the fundamental transverse electric mode in a structure similar to Fig. 1(c) with a laser mesa width of $w_a = 5 \mu\text{m}$, tantalum width of $w_f = 500 \text{ nm}$, and height of $h_f = 300 \text{ nm}$ is shown in Fig. 1(d). About 6% of the optical power is confined within the two quantum wells.

3. Characterization

The laser devices are characterized by applying continuous current to the laser diode (see Fig. 2 (a)), while the output power is measured using a wide-area photodetector. The voltage across the laser contacts is also monitored at different applied current levels to record the diode-type behavior of the laser device. During the optical and electrical characterization of the devices, the laser chip is mounted on a copper stage, the temperature of which is controlled using thermo-electric coolers.

The LIV-curve for a DFB laser with an active length of $L_a = 450 \mu\text{m}$, a laser mesa width of $w_{\text{mesa}} = 5 \mu\text{m}$, at a stage temperature of $20 \text{ }^\circ\text{C}$ is shown in Fig. 2(b). The corresponding optical spectrum of the DFB laser at 25 mA and 30 mA driving current is shown in Fig. 2(c) with blue and red curves, respectively. The threshold current in Fig. 2(b) is 14 mA, and the maximum power of 5 mW per facet (with two ideally identical facets) is achieved in a continuous-wave (CW) single-mode laser at free space wavelength of $\lambda = 1020 \text{ nm}$, with a side-mode suppression ratio of 22 dB. The single-mode operation of the laser indicates the interaction of the tantalum PIC with the gain layer in the III-V epitaxial stack.

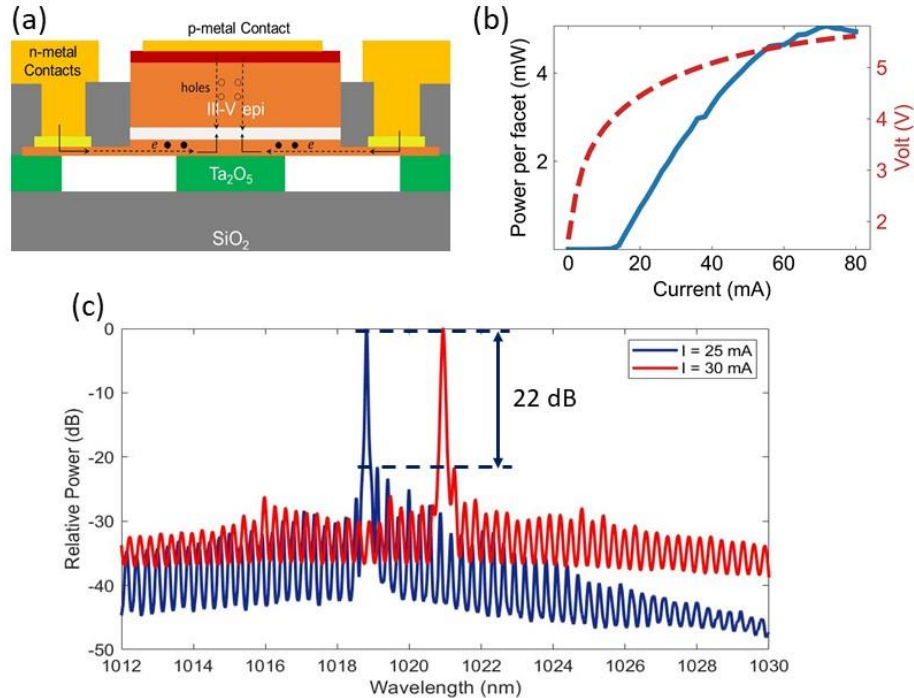


Figure 2. (a) Cross-section schematic of the heterogeneously integrated laser. The black arrows indicate the laterally injected current flow from the *n*-type to the *p*-type contacts with (b) LIV-curve and (c) the optical spectrum of the DFB laser at a stage temperature of 20 °C. The active length of the DFB laser is $L_{\text{active}} = 450 \mu\text{m}$, and the laser mesa width is $w_{\text{mesa}} = 5 \mu\text{m}$. The optical spectrum of the DFB laser is shown at two different driving currents of 25 mA and 30 mA (resolution bandwidth is 0.05 nm). The side-mode suppression of the single-mode DFB is 22 dB.

4. Conclusion

The first heterogeneous DFB diode laser based on the integration of an InGaAs QW gain layer and patterned tantalum photonic integrated circuitry is demonstrated at a near-infrared wavelength of 1020 nm. The DFB laser features a low threshold current of 14 mA and maximum output power of 5 mW per facet (with two ideally identical facets) in a 450 μm long DFB laser with a side-mode suppression ratio of 22 dB. The laser fabrication leverages a wafer-scale integration of a III-V InGaAs active layer with a passive tantalum PIC on a single Si substrate through low-temperature direct wafer bonding with high area yield.

5. Acknowledgement

This work was supported by the DARPA LUMOS program.

6. References

- [1] Liang, D. and Bowers, J.E., 2021. Recent progress in heterogeneous III-V-on-silicon photonic integration. *Light: Advanced Manufacturing*, 2(1), pp.59-83.
- [2] Xiang, C., Jin, W., Guo, J., Peters, J.D., Kennedy, M.J., Selvidge, J., Morton, P.A. and Bowers, J.E., 2020. Narrow-linewidth III-V/Si/Si₃N₄ laser using multilayer heterogeneous integration. *Optica*, 7(1), pp.20-21.
- [3] Cha, J., Shin, D., Shin, Y., Cho, K., Ha, K., Lee, K. and Kang, H.K., 2019, July. Heterogeneous Integration of O-band LDs on bulk-Si Platform. In 2019 24th OptoElectronics and Communications Conference (OECC) and 2019 International Conference on Photonics in Switching and Computing (PSC) (pp. 1-3). IEEE.
- [4] Tran, Minh A., Chong Zhang, Theodore J. Morin, Lin Chang, Sabyasachi Barik, Zhiquan Yuan, Woonghee Lee et al. "Extending the spectrum of fully integrated photonics to submicrometre wavelengths." *Nature* (2022): 1-7.
- [5] Dorche, Ali Eshaghian, Nima Nader, Eric J. Stanton, Sae Woo Nam, and Richard P. Mirin. "High-quality factor tantalum pentoxide microring resonator mirror at 780 nm." In 2022 Conference on Lasers and Electro-Optics (CLEO), pp. 1-2. IEEE, 2022.
- [6] Dorche, Ali Eshaghian, Bochao Wei, Chandra Raman, and Ali Adibi. "High-quality-factor microring resonator for strong atom-light interactions using miniature atomic beams." *Optics Letters* 45, no. 21 (2020): 5958-5961.